



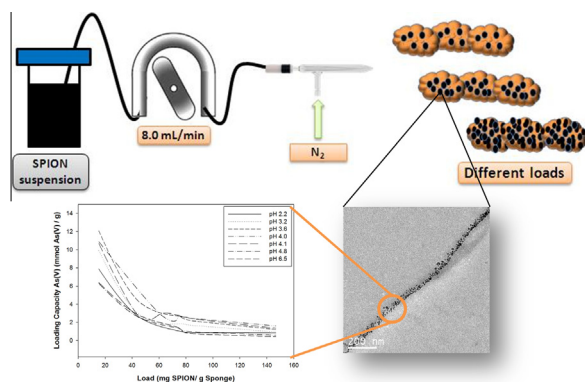
Efficient arsenic(V) and arsenic(III) removal from acidic solutions with Novel Forager Sponge-loaded superparamagnetic iron oxide nanoparticles

D. Morillo*, G. Pérez, M. Valiente

Universitat Autònoma de Barcelona, Centre GTS, Department of Chemistry, 08193 Bellaterra (Barcelona), Spain



GRAPHICAL ABSTRACT



ARTICLE INFO

Article history:

Received 24 March 2015

Accepted 24 April 2015

Available online 4 May 2015

Keywords:

Arsenic removal

Superparamagnetic iron oxide nanoparticles

SPION

Forager Sponge

ABSTRACT

Nowadays, there is a wide variety of arsenic decontamination processes being adsorption processes the most efficient. In this concern, superparamagnetic iron oxide nanoparticles (SPION) have been proposed as an appropriate system to improve arsenic adsorption from acidic wastewater. The number of mines, the amount of ore processed, and thus the amount of mine (acid) wastewaters have been rapidly increased in recent decades. For this reason, arsenic removal from contaminated water is an important goal to accomplish environmental regulations. It is noteworthy that aggregation of these nanoparticles has been detected as the main difficulty, hindering the promising adsorption. In order to overcome this drawback, it is proposed a system to avoid aggregation based on nanoparticles dispersion into an appropriate supporting material. To this purpose, SPION have been fixed on a cellulosic sponge achieving a decrease of the aggregation state, an increase of the active centers, and consequently, arsenic adsorption increases. Experimental results report a lower aggregation of supported SPION over sponge than the observed in the non supported nanoparticles. At this point, a remarkable improvement in the sponge system adsorption capacity is observed in comparison with superparamagnetic nanoparticles in suspension, reaching adsorption capacities about 2.1 mmol As/g SPION and 12.1 mmol As/g SPION for arsenite and arsenate, respectively at pH 3.8. Then, the developed system not only amends the aggregation problem but also keep their nanoproperties intact, making the system a suitable one for arsenic removal in acidic wastewater treatment.

© 2015 Elsevier Inc. All rights reserved.

* Corresponding author. Fax: +34 937891906.

E-mail addresses: Diego.morillo.martin@gmail.com (D. Morillo), Gustavo.perez@uab.es (G. Pérez), manuel.valiente@uab.es (M. Valiente).

1. Introduction

Arsenic is a relatively scarce but ubiquitous element, with environmental substrates showing ranges of arsenic concentrations from ppb to ppm levels [1]. The impact of both natural and anthropogenic inputs of arsenic species in the environment, mainly in soils and waters, is considered to be one of the major problems in pollution abatement, because of their high toxicity and the consequent risks for human health [2].

The oxidation state of arsenic plays an important role since it determines the properties of the related species, i.e., the toxicity, the sorption behavior and the mobility in the aquatic environment. However, in natural waters arsenic is found mostly as As(III) and As(V) [3]. The World Health Organization has reduced the MCL (Maximum Contaminant Level) from 50 µg/L to 10 µg/L [4,5]. Thus, there is a growing interest in using low-cost methods and materials to remove arsenic from industrial effluents (mainly mine industry) before it may cause significant contamination.

The increasing number of operating mines raises concerns for health and environment, and many of those concerns are related to mine water issues [6]. Mining operations often produce substantial amounts of acidic wastewater which contain highly elevated concentrations of potentially harmful substances including trace metals and metalloids (e.g., nickel (Ni), arsenic (As), lead (Pb) or antimony (Sb)) [7].

Although multiple methods such as precipitation [8], ion exchange [9] or membrane processes [10] have been used for arsenic removal, selective adsorption [11] from solution has received more attention due to its high concentration efficiency. Bulk iron oxides have demonstrated their affinity for arsenic but iron oxide nanoparticles provides an advantage due to an increase of the surface-volume ratio and specific surface area, allowing more active sites to better improve the adsorption process [12]. Small size gives nanoparticles a high surface area to volume ratio, a high surface reactivity, new properties such as electrical, magnetic, optical, and chemical. In this sense, the interaction with different kinds of chemical species offers better kinetics for selective sorption of ions from aqueous media [13]. At the nanoscale, inorganic metal oxides are potentially highly efficient agents for binding ions such as those of some pollutants (i.e. arsenic). By tailoring the composition of the metal oxides, selective adsorption of different ions can be introduced, becoming the use of nanoparticles a very attractive new adsorption area for the recovery of ions from industrial wastes.

A literature survey identifies different nano-size iron oxides structures such as maghemite ($\gamma\text{-Fe}_2\text{O}_3$) [14], siderite (FeCO_3) or fougérite ($(\text{Fe(II)}_4\text{Fe(III)}_2(\text{OH})_{12})[\text{CO}_3\cdot 2\text{H}_2\text{O}]$) being used to study the adsorption mechanisms and the extent of adsorption of arsenic ions [15–17]. Additionally, other materials for arsenic adsorption such as resins or loaded iron (III) sponges have been found [18]. Its noteworthy that the surface chemistry of the iron oxides has a pH-dependent charge. At low pH, the hydroxyl groups at the surface of the iron oxide are doubly protonated ($-\text{FeOH}_2^+$) and the surface charge of the iron oxide is thus positive. At a certain pH, the hydroxyl group is protonated with only one proton ($-\text{FeOH}$) and thus the (net) surface charge of the iron oxide is neutral. This pH is called the point of zero charge (PZC) and for iron oxides the point of zero charge (PZC) ranges between 5.5 and 9.8 (in case of SPION pzc is 6.8). At pH values above the PZC, the hydroxyl group is deprotonated ($-\text{FeO}^-$), and consequently the iron oxide surface bears a negative charge. Then, under those conditions the SPION surface had different charge properties (positive, neutral or negative).

The objective of the present work is to investigate the role and the effectiveness of nanosized magnetic particles, specifically, superparamagnetic iron oxide nanoparticles (SPION) in the adsorption of arsenic(V) and arsenic(III) ions from acidic aqueous media.

In order to demonstrate the feasibility of using SPION for the binding and removal of both arsenic species, these nanoparticles will be supported over a commercial ion exchange material (Forager Sponge) based on an open-celled cellulose sponge.

2. Experimental section

2.1. Chemicals and reagents

Analytical grade solution of iron(III) chloride hexahydrate, iron(II) chloride anhydrous, ammonium hydroxide, sodium acetate trihydrate, acetic acid, sodium hydrogen arsenate heptahydrate, sodium metaarsenite and hydrochloric acid were used. An open celled cellulose sponge with an amine-containing polymer which presents a nominal particle size of 12.7 mm (Forager Sponge, Dynaphore) was used as SPION support. Tetramethyl ammonium hydroxide (TMAOH, Fluka 25%) was used as redispersing agent and high purity water with a resistivity of 18 MΩ/cm was used throughout all the experiments.

2.2. Characterization of adsorbent materials

Two types of adsorbent materials were used to remove arsenic from contaminated solutions. Superparamagnetic iron oxide nanoparticles (SPION) were imaged with a transmission electron microscopy (TEM, JEOL JEM-2011 HRTEM). The crystallographic phase was also undertaken by analyzing the X-ray powder diffraction spectra (XRD, X-Pert Philips diffractometer), using a monochromatized X-ray beam with nickel-filtered Cu K α radiation ($\lambda = 0.154021$ nm). The magnetization of both SPION and adsorbed SPION over cellulose was determined by Superconducting Quantum Interference Device (SQUID, MPMS-XL 7T) [19–21]. Forager Sponge loaded SPION was characterized by TEM. Iron content was determined in order to control nanoparticles in the solution by inductively coupled plasma atomic emission spectroscopy (ICP-OES, Intrepid II, Thermo Fisher). The results reveal an iron content in all samples below the detection limit of the equipment (1 ppb). This content confirms the SPION stability in all the performed experiments and no leaching is produced from the sponge surface.

2.3. Synthesis of adsorbent materials

The synthesis of 10 nm SPION was performed as described elsewhere [22,23], with some modifications to increase the reaction yield. The synthesis requires a constant bubbling of nitrogen to prevent oxidation of Fe^{2+} to Fe^{3+} . A stock solution of Fe^{3+} in a chloride medium was prepared by dissolving $\text{FeCl}_3\cdot 6\text{H}_2\text{O}$ in a deoxygenated HCl 0.2 M solution. A stock solution of NH_4OH 0.7 M was deoxygenated under nitrogen atmosphere and heated to 70 °C. Later on, Fe^{3+} solution was added to the deoxygenated NH_4OH solution. After few minutes, anhydrous FeCl_2 was added, in a ratio 1:2 of $\text{Fe}^{2+}/\text{Fe}^{3+}$. Then, the solution was kept 45 min under mechanical stirring and nitrogen bubbling for the ageing of nanoparticles. After sample cooling, the resulting suspension was centrifuged at 2000 rpm, separating the nanoparticles by a magnet and washing with deoxygenated water several times. A subsequent redispersion in deoxygenated aqueous solution of tetramethylammonium hydroxide (TMAOH) 0.01 M (pH \approx 12) let to obtain SPION in a stable suspension for 6–8 months under deoxygenated atmosphere.

2.4. Synthesis of the Forager Sponge-loaded SPION material

After SPION synthesis, Forager Sponge was loaded with SPION to develop a new adsorbent material. A pretreatment, by

immersion in a hydrochloric acid for wiping their acidic form [18], was performed in order to activate the amino groups and to facilitate SPION immobilization. Once in protonic form, Forager Sponge was dried during 24 h at 40 °C in oven and introduced in a desiccator until their use.

Once the Forager Sponge is in acidic form, SPION load on the Forager Sponge surface was performed. Such surface immobilization was achieved using a pneumatic nebulizer that generates a homogeneous SPION dispersion spray, with the assistance of a peristaltic pump, under nitrogen stream.

Variation on the amount of SPION concentration and also the nebulisation time produced different SPION immobilization and different SPION load on sponge surface. Finally, a cleaning process was needed with nitrogen saturated water in order to remove the SPION excess that was not attached over the sponge surface. Forager Sponge loaded SPION was dried during 24 h at 40 °C in oven and is kept in a desiccator until their use.

2.5. Adsorption–desorption experiments over SPION and Forager Sponge-loaded SPION

The adsorption experiment was performed in batch mode by mixing aqueous solution of As(V) and/or As(III) in acetic/acetate 0.2 mol/L media with constant aliquots of SPION (50 mg) or Forager Sponge-loaded SPION (50 mg) using a rotatory shaker at room temperature. The pH of the solution ranged between 1 and 8 (depending of the experiment) was controlled using either HNO₃ or NaOH standardized solutions and confirmed by pH measurements. After mixing, the solid phase was removed from the supernatant by decantation with magnet force and filtration with cellulose acetate filters of 0.22 μm. The final pH was measured as the pH value of the experiment and this value was used as pH value in all the adsorption experiments.

The adsorption capacity (q_{As} , mmol/g) is determined measuring the initial ($C_{As\ ini}$, mmol As/L) and equilibrium ($C_{As\ fin}$, mmol As/L) arsenic concentration for each experiment and applying the equation (L):

$$q_{As} = \frac{V_{ads} \cdot (C_{As\ ini} - C_{As\ fin})}{m_{ads}} \quad (1)$$

where V_{ads} is the volume of reaction (L) and m_{ads} is the adsorbent quantity (g).

In the desorption experiments, 10 mL of the elution solution were added to an accurately measured quantity of Forager Sponge-loaded SPION with As(V) and/or As(III) adsorbed using a rotatory shaker at room temperature. After 60 min of contact, the aqueous and the solid phases were separated by centrifugation and the concentration of arsenic in the supernatant was measured.

The concentration of metal ions in the supernatant was determined by inductively coupled plasma atomic emission spectroscopy (ICP-AES, iCAP 6000, Thermo Fisher, Waltham, MA, USA). Arsenic(V) and arsenic(III) adsorption was calculated by mass balance and the effect of different parameters was recorded. Additionally, iron content was determined to control the stability of SPION in the experimental media during the adsorption experiments and the results reveal an iron content below the detection limit of the equipment (1 ppb). This content confirms the SPION stability in all the performed experiments.

2.6. Anion selectivity experiments

Experiments were performed to study the anion selectivity of the adsorbent system. The experiments were carried out with solutions of As(V) containing 0.25 mol L⁻¹ of Cl⁻, NO₃⁻, SO₄²⁻ or PO₄³⁻ (ratio 20:1 respect of As(V) total in solution) were treated to observe the behavior of the adsorbent system in the presence of

interfering anions. The experiments were performed in the same way as the adsorption experiments by mixing a known amount of Forager Sponge-loaded SPION with the solutions using rotary shaker at room temperature (23 °C). The pH of the solution was controlled using either HNO₃ or NaOH standardized solutions and confirmed by pH measurements.

3. Results and discussions

3.1. Characterization of adsorbent materials

The characterization of nanoparticles morphology, mainly its size that determines their adsorption capacity, requires from TEM measurements. A review of the actual existing literature highlights an optimal particle size range between 8 and 10 nm for adsorption applications [17,24]. From the TEM micrographs (Fig. 1) a main spherical nanoparticles morphology can be observed, being partially aggregated when SPION are in suspension. The main nanoparticle size obtained by using the described synthesis method has an average size of 10.2 nm

The SPION dispersed over the Sponge surface was characterized using the same characterization techniques. Fig. 2 shows the TEM micrographs of the Forager Sponge loaded SPION cross section and indicate that a greater specific surface is achieved with an adequate optimization of the SPION dispersion process, and therefore, greater adsorption capacity could be obtained in SPION loaded Forager Sponge due to the high dispersion of SPION.

In order to characterize the SPION distribution on the sponge, different deposition ways were developed, such as Forager Sponge impregnation by dipping for 24 h in SPION suspension or spray this suspension by pneumatic nebulizer. These tests reveal that longer dipping processes (Fig. 2a) produce a higher aggregation of SPION than using a pneumatic nebulizer (Fig. 2b–d). Thus, with a low loading (20 mg SPION/g Sponge), a homogeneous and uniform SPION distribution on the Forager Sponge surface was observed, not achievable at a high loading (140 mg SPION/g Sponge).

These loading properties will result of key importance for the As(III) and As(V) adsorption process efficiency on SPION. Theoretically, the decrease of SPION aggregation generates an increase of the specific surface area and therefore an increment in the reactive centers on the adsorbent material for the adsorption process of As(III) and As(V).

Superparamagnetic materials have no permanent magnetic moment and, hence, no hysteresis loop. To test the magnetic susceptibility, the temperature was held constant at 300 K for hysteresis measurements at the applied field ±7 T, see Fig. 3. The shape of the hysteresis curve for the sample was normal and tight with no hysteresis losses, typical behavior of superparamagnets. Under low applied field, a high magnetization (M) value was observed. The saturation magnetization (M_s) and the coercivity (H_c) of the SPION are about 80 emu/g and 143 Oe respectively, values close to bulk Fe₃O₄ (85–100 emu/g and 115–150 Oe, correspondingly). Accordingly to the observed remaining magnetic capacity, together with the high specific surface areas and strong magnetic properties, SPION appears as an excellent adsorbent candidate for environmental applications.

The shape of the hysteresis curve for Forager Sponge loaded SPION the sample was normal and tight with no hysteresis losses. Under low applied field, a high magnetization value was observed similarly to SPION. The saturation magnetization and the coercivity of the SPION loaded Forager Sponge are about 30 emu/g and 48 Oe, respectively. Taking into account that 2 mg of sample were needed for the determination and the SPION loaded Forager Sponge has a concentration of 20 mg SPION/g Forager Sponge, the obtained

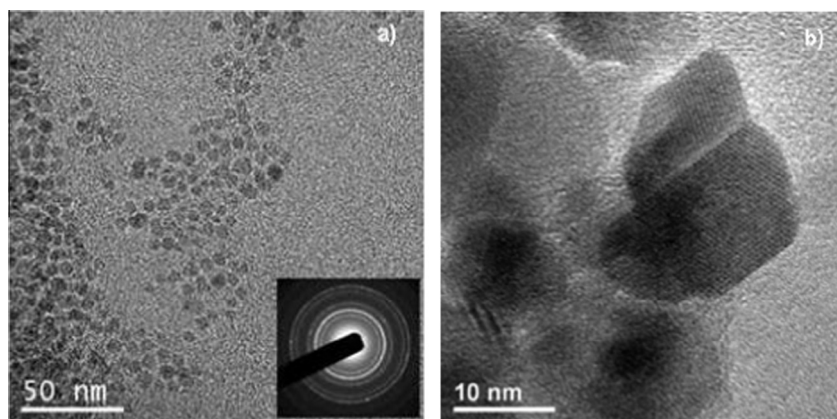


Fig. 1. TEM micrograph of synthesized SPION with its diffractogram (a) and TEM micrograph at high resolution (b).

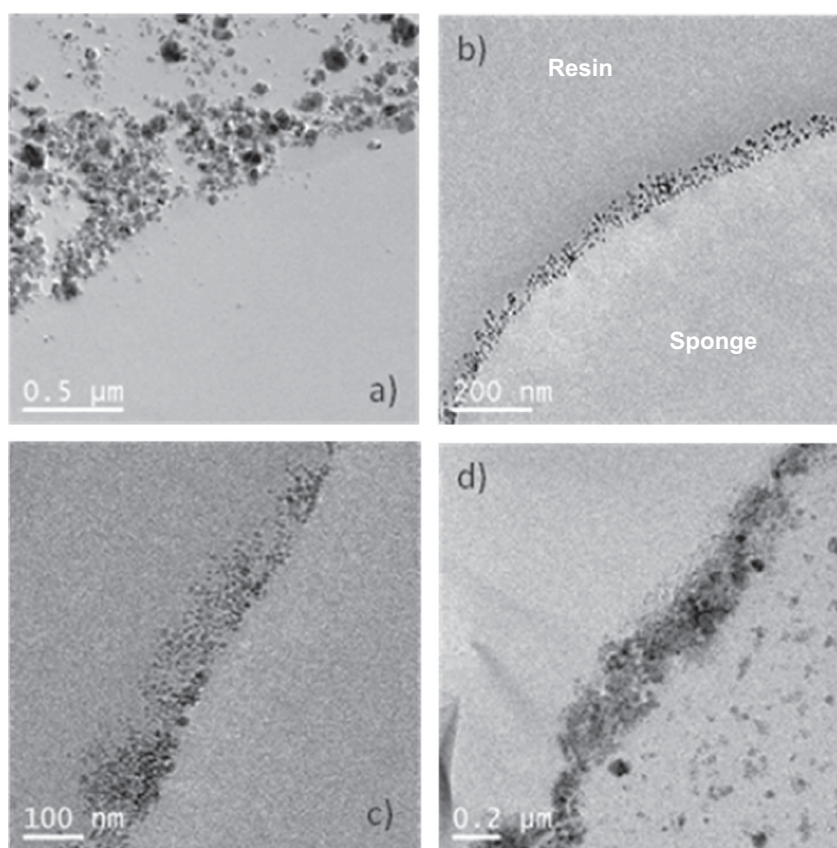


Fig. 2. TEM micrograph of the cross sections for the different Forager Sponge loaded SPION samples. Loading by dipping during 24 h (a), low (b), intermediate (c) and high load (d) of SPION over the sponge surface.

values reflected that despite the lower amount of SPION over the sponge surface if compared with the SPION powder, the SPION still retained their magnetization. Thus, reveal a remaining magnetic capacity of interest in order to recover the product when treating contaminated solutions.

3.2. As(V) and As(III) adsorption kinetic over SPION

In these experiments the effect of contact time on the adsorption were studied. The experiments were carried out by mixing 100 mg L⁻¹ solution of either As(III), As(V) or As(III)/As(V) mixtures (100 mg L⁻¹ As(III) + 100 mg L⁻¹ As(V)) with a constant amount of SPION, working at room temperature (23 °C) and pH range 2.4–4.5 with the contact time varying in the period of 1–60 min. In the case

of arsenate, the variation of its adsorption with time, independently of pH effect, is relatively fast, as seen in Fig. 4a, where longer contact time provide no significant variations in the adsorption capacity of the SPION. The results of the interaction between the arsenate solutions and the SPION suspension at different pHs show that arsenate adsorption is highly pH dependent. The increase of deprotonated arsenic species by increasing the pH in the range of 2.8–3.8 is the reason of the observed increase on the adsorption capacity in this range of pH. At higher pH values, the competition of OH⁻ ions against arsenate to complex Fe(III) lead to a decrease of the arsenate adsorption.

On the other hand, in the case of arsenite, the dynamics of the adsorption process is observed to be in a similar way of arsenate. However, in this case, the adsorption is independent of pH (see

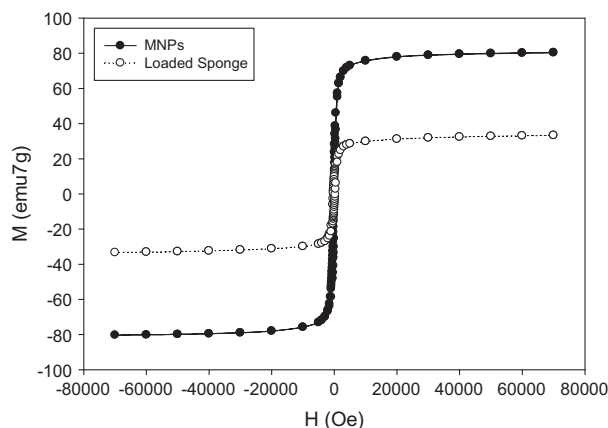


Fig. 3. The M vs H dependence for SPION and SPION loaded Forager Sponge at 300 K.

Fig. 4b) what corresponds to the less acidic properties of arsenious. This leads to the observed almost constant arsenite adsorption capacity with pH.

When using monocomponent solutions, the maximum adsorption capacity values obtained at stationary state, at pH 3.8, were found to be 0.91 mmol As(V)/g SPION and 0.43 mmol As(III)/g SPION, respectively.

The results for adsorption processes in presence of both arsenic species given in Fig. 5 reveal a competition between both species. This competition explains the adsorption values closer to As(V) behavior (expected from its better interaction with SPION) being the achieved adsorption capacity at the stationary state 0.66 mmol As/g SPION. The observed decrease in the adsorption is due to the less concentration of As(V) in the target solutions.

3.3. Effect of pH on the adsorption capacity over un-supported SPION

These experiments were carried out by mixing 100 mg L⁻¹ solution of either As(III), As(V) or As(III)/As(V) (100 mg L⁻¹ As(III) + 100 mg L⁻¹ As(V)) mixtures with a constant amount of SPION at room temperature (23 °C) during 120 min to reach stationary state. A pH range 2.0–8.0 (after the adsorption process) was studied in order to identify the optimum adsorption pH.

Arsenite and arsenate SPION adsorption capacity varies according to the experimental pH as illustrated in Fig. 6. Arsenate adsorption is strongly influenced by the pH, especially at low pH values where the acidity of arsenate species ($pK_{a1} = 2.2$) produce

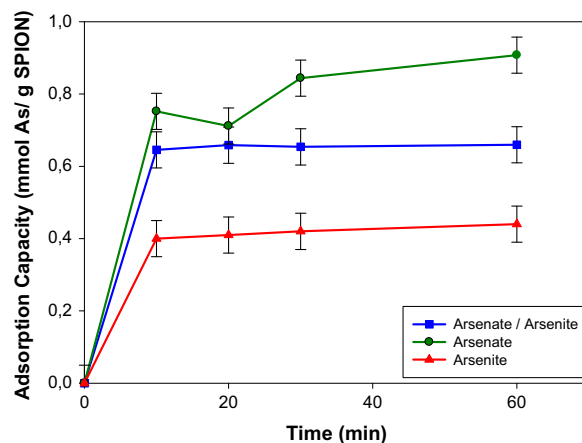


Fig. 5. SPION kinetic adsorption for As(III)/As(V) mixtures at pH 3.8.

deprotonated species, is responsible of the observed relatively high adsorption capacity in the pH range 2.0–3.8. With the increase of pH above the indicated range, competition between OH⁻ and As(V) ions for Fe(III) centers increases and it leads to that the observed decrease on the adsorption of arsenate.

For arsenite, the situation is completely different. Less acidity of arsenite species ($pK_{a1} = 9.2$) as well as the reduced presence of deprotonated arsenite species in the pH range of study produces a non-significant pH effect.

When analyzing As(III)/As(V) mixtures, the shape of the figure presents competitiveness between both arsenite and arsenate. This competitiveness shows certain pH dependency due to the arsenate adsorption. Arsenate is more acid than arsenite (there is an unique specie at the studied pH range, H₃AsO₄) thus adsorption capacity of mixtures changes in the same way than arsenate solutions. These results suggest that, taking into account the related results for the individual species, arsenite is also adsorbed but in much less proportion than arsenate. Then, a decrease in the total arsenic adsorption is generated respect the adsorption capacity reached with only arsenate present.

3.4. Maximum SPION adsorption capacity

These experiments are planned to assess the effect of the initial arsenite or arsenate concentration on the sorption process and estimate the maximum SPION adsorption capacity for both species, verifying if further optimization of maximum adsorption capacity can be achieved. Initial arsenic concentration in the range of

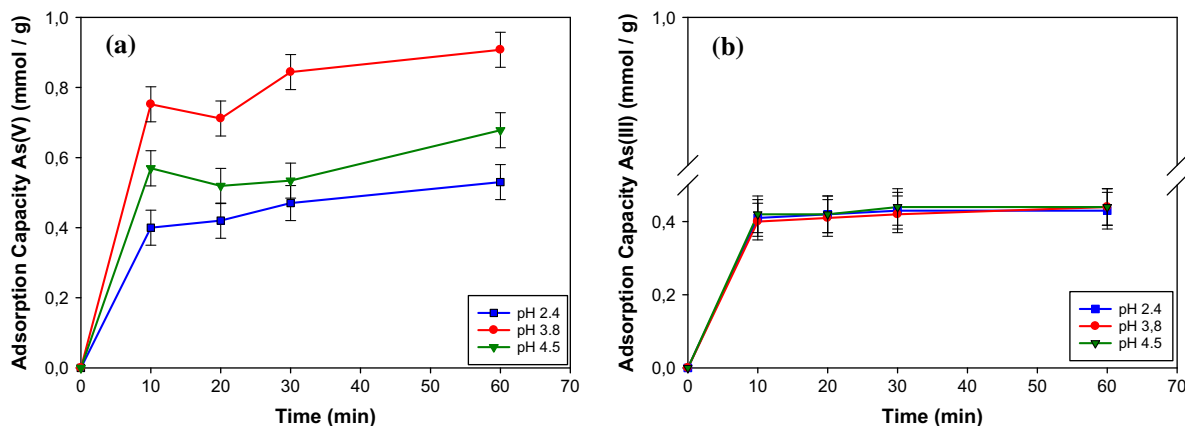


Fig. 4. SPION kinetic adsorption capacity at different pH: As(V) (a), As(III) (b). The lines are guidelines.

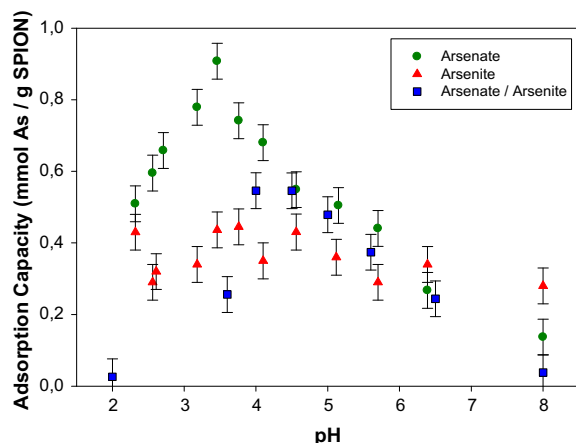


Fig. 6. pH effect for As(V) and As(III) adsorption on SPION suspensions.

1 mg L⁻¹ and 1000 mg L⁻¹ were tested under room temperature (23 °C) during 120 min. The relationship between the equilibrium aqueous concentration and the equilibrium adsorption capacity for arsenite and arsenate, shown in Fig. 7, fits Langmuir adsorption model, as follows Eq. (2):

$$q_e = \frac{q_{\max} k_L C_e}{1 + k_L C_e} \quad (2)$$

That can be written as:

$$\frac{C_e}{q_e} = \frac{1}{q_{\max} k_L} + \frac{C_e}{q_{\max}} \quad (3)$$

where q_e is the equilibrium adsorption capacity (mmol/g), C_e is the equilibrium metal concentration in the aqueous phase (mmol/L), q_{\max} is the maximum loading capacity (mmol/g) corresponding to a monolayer coverage, and k_L is Langmuir constant (L/mol).

For both arsenite and arsenate, the adsorption capacity increases with the initial concentration due to the saturation effect. For arsenate, optimal adsorbent working conditions are reached at pH 3.6, providing a saturation of arsenate adsorption capacity near 0.91 mmol As(V)/g SPION. The minimum arsenate concentration needed for the saturation is 500 mg L⁻¹, representing the extreme working conditions, in terms of concentration, that can face the adsorbent. The SPION works similarly in the case of arsenite but reaching a maximum adsorption capacity of 0.43 mmol As(III)/g SPION being 100 mg L⁻¹ of arsenite needed to saturate the system. The experimental model fits Langmuir model as indicated in Fig. 8,

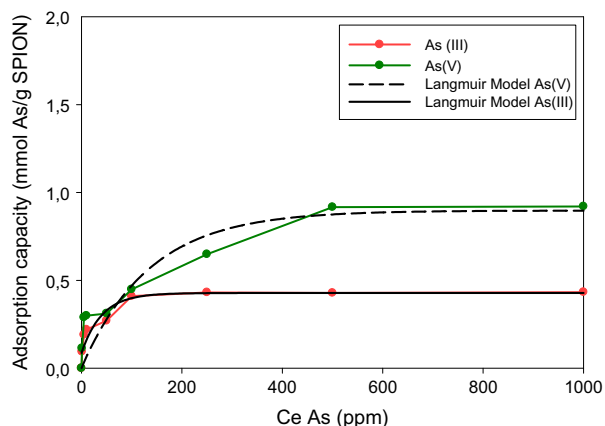


Fig. 7. Effect of initial As(V) and As(III) concentration.

being 8.52 L/mol and 1.57 L/mol for arsenite and arsenate, respectively.

3.5. pH effect in the adsorption of As(V) and As(III) over Forager Sponge-loaded SPION

The study and determination of adsorption capacity of the Forager Sponge-loaded SPION was performed analogous to the procedure described for adsorption on SPION.

The adsorption of the different arsenic species using Forager Sponge-loaded SPION was investigated by varying the solution pH in the range 2–7 (after the adsorption process) taking into account that for the previous studied materials. The obtained results (Fig. 9a) revealed that the adsorption of As(V) is pH dependent and As(III) is pH independent. Such behavior can be explained by the presence of different As(III) and As(V) forms in the aqueous solution at different pHs. Additionally, Forager Sponge presents a very small arsenite and arsenate adsorption which is important to determine the adsorption capacity of SPION loaded in the system. In this case, Forager Sponge is just a support without interference in the adsorption process.

A comparison of the observed pH effect with that obtained on previous As(V) adsorbent, non-supported SPION alone, revealed similar behavior with an adsorption maximum at pH 3.8. In addition, the amount of SPION loaded on the Forager Sponge was considered. In this case, three different SPION loadings were generated by pneumatic nebulization over the Sponge, low (44.5 mg SPION/g Sponge), intermediate (84.2 mg SPION/g Sponge) and high loading (146.7 mg SPION/g Sponge). In all these situations the pH influence is similar, achieving a pH of maximum adsorption capacity at 3.6–3.8.

The observed higher adsorption capacity for the low loading SPION is due to the higher dispersion of SPION on the sponge, what provides higher specific surface area that will increase the adsorption rate of arsenite in SPION.

For arsenite, SPION loaded Forager Sponge presents a completely different situation (Fig. 9b) due to the absence of adsorption capacity variation within the target pH range. Such behavior follows the observed for non-supported SPION. As in that case, the less acidity of arsenite species ($pK_{a1} = 9.2$) is the reason for such non-significant pH effect.

In this sense, the ion exchange and the adsorption of both forms of arsenic is possible at any pH range, with a maximum of 0.3 mmol As(V)/g Sponge within the pH range (3–5). Moreover, only in basic solutions, As(III) may dominate. Under the working pH conditions, the operational capacity of the sponge is very small

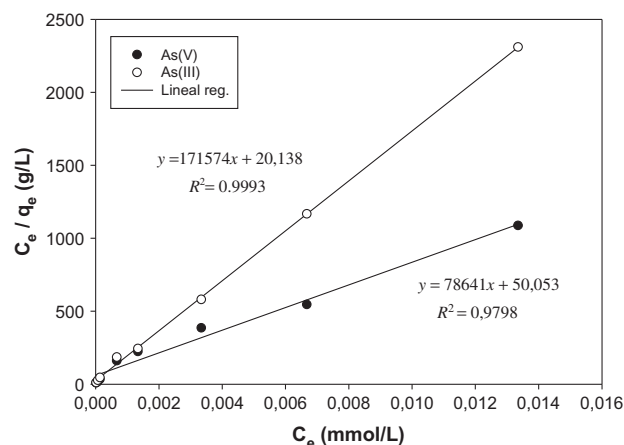


Fig. 8. Fitting experimental data for the Langmuir model.

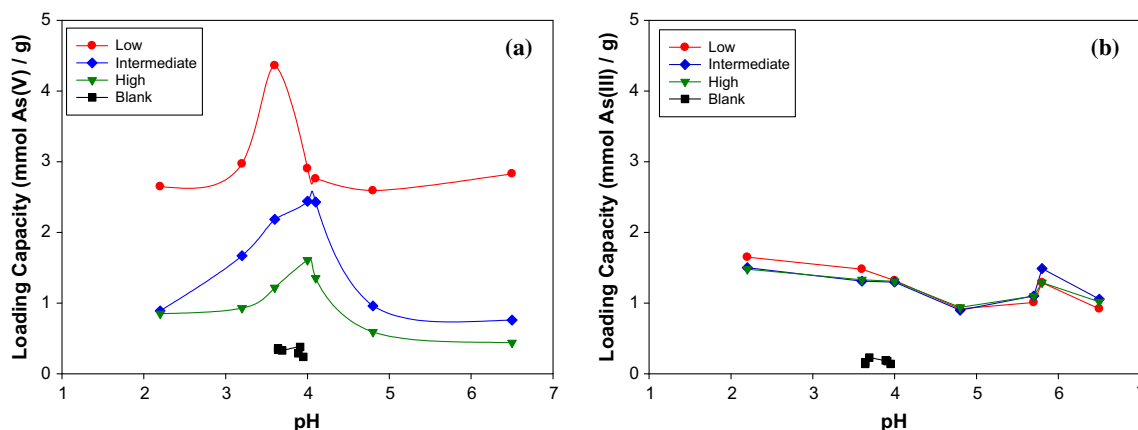


Fig. 9. pH effect over As(V), (a) and As(III), (b) Forager Sponge loaded SPION adsorption capacity.

(0.15 mmol As(III)/g sponge), being the adsorption of As(III) on sponge very low in all the pH range.

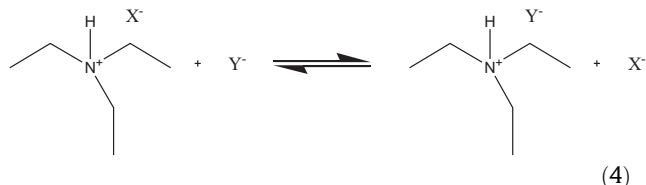
3.6. SPION load effect in the adsorption of As(V) and As(III) over Forager Sponge-loaded SPION

The effect of the of SPION amount loaded on the Forager Sponge on the adsorption capacity of As(V) and As(III), was studied with the optimized time conditions (60 min) and in a wide pH range to evaluate the behavior in the target pH range 2.2–6.5 as shows Fig. 10.

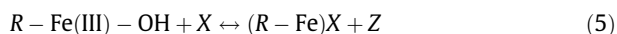
The high number of ethylamine groups on the Sponge surface makes the blank Forager Sponge to show high acidity, and it explains the ability of the blank Forager Sponge to adsorb and immobilize Fe(III) from the SPION by *chelation* through the lone pairs of electrons on the unprotonated amine groups, as the triethylenetetramine favorably complexes Fe(III).

In all situations, the observed behavior can be interpreted based on two differentiated types of interactions. In one hand, an anion exchange of arsenic species corresponding to the protonated amine groups present in the matrix of the Sponge. However, there is a second process where a ligand exchange, provided by the Fe(III) ions immobilized in the SPION is promoted [25]:

- (a) The first interaction, as show the following Eq. (4), involves an anion exchange of arsenic species corresponding to the protonated amine groups present in the matrix of the sponge. This interaction will be dependent of the equilibrium pH of the aqueous solution, where Y is the species of arsenic exchanged by the counter ion (X).

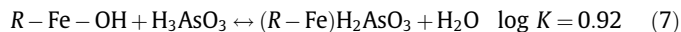
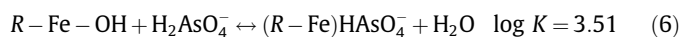


- (b) There is a second process where an exchange of ligands provided by the Fe(III) ions of the SPION immobilized in the supporting material, Forager Sponge, is promoted. This can be expressed by the general Eq. (5):



where R is the matrix of the SPION, X is the chemical species of arsenic at the optimal pH and Z is the exchanged ligand, OH[−] ions in the case of As(V) and H₂O for As(III). The affinity of arsenic oxoanions for the iron on SPION is higher for the Fe(III) ions than Fe(II) ions. This provides a higher activity of the Fe(III) ions with OH[−] than Fe(II) ions.

As mentioned above, the differential behavior of both arsenic species is related to the different acidity of their respective oxoanions [26]. While H₃AsO₄ is a strong, H₃AsO₃ is a very weak one. This generates the existence of an As(V) oxoanions in solution, which will be adsorbed on the sponge by the protonated amine groups from a relatively acidic pH to basic pH values. Moreover, the difference in adsorption between the blank sponge and the SPION loaded Forager Sponge it is attributed to the presence of Fe(III) ions in the nanoparticles, which provide exchange adsorption centers for arsenic species. In this sense, the processes occurring during the arsenite and arsenate adsorption, at the studied pH, on SPION loaded Forager Sponge, could be explained by these Eqs. (6) and (7) [27]:



With these calculated data, that follow the tendency of similar adsorption reactions, and if we assume the ligand exchange model expressed before, the adsorption of As(V) on the SPION loaded Forager Sponge is favoured over the adsorption of As(III), similarly to the adsorption observed over other iron oxides [28,29].

The presence of SPION immobilized in the sponge enhances the adsorption capacity of both arsenic species with respect to the non-supported SPION, so that the maximum adsorption of the sponge is 12.09 mmol As (V)/g SPION at initial pH 3.6 and 2.11 mmol As (III)/g SPION at pH 4.0. This range confirms the optimum pH for maximum adsorption obtained for arsenic adsorption on SPION suspension. This fact, coupled with the reduced adsorption of As(III) throughout the studied pH range, shows the possibility of separating both arsenic species.

3.7. Anions interference on SPION selectivity

Anions commonly present in wastewaters such as chloride, nitrate, sulfate or phosphate, potentially interfere the arsenic adsorption, being such interference very significant leading to a

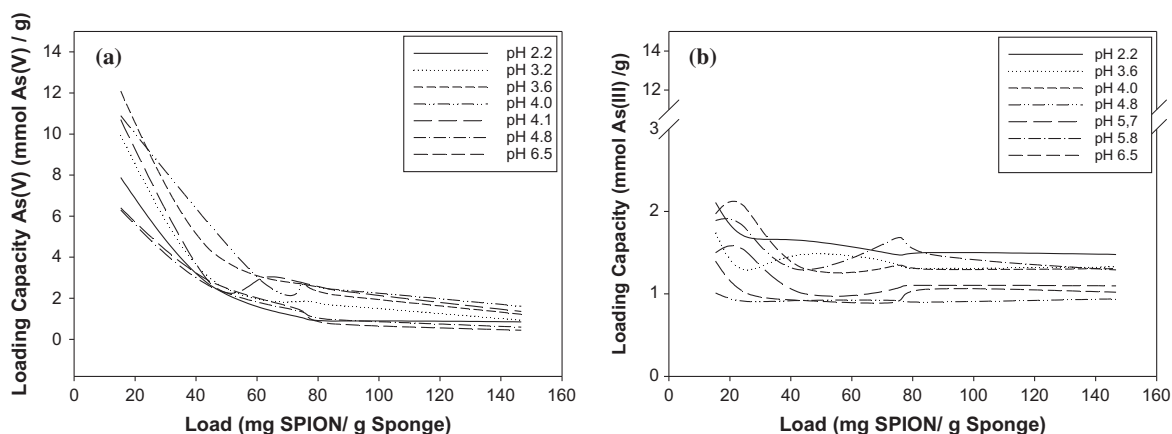


Fig. 10. Adsorption capacity for SPION loaded sponge with different loads: (a) As(V) and (b) As(III).

reduction of the arsenic adsorption capacity. The general trend previously observed for arsenic adsorption is varying the adsorption capacity with the pH, being similar when different anions are present.

When anions are present in the arsenic solution, arsenic adsorption has remarkable decrease. The adsorption capacity at low and high studied pHs increases due to the presence of interfering anions favor the anionic environment on the anion exchange centers leading to an easier anion exchange process. At the maximum adsorption pH (4.0), the presence of different anions in high quantity, especially phosphate, produce an efficient competition with arsenic in the ligand exchange centers of the SPION. This fact is consequence of the similar affinity for phosphate and arsenate. For the other anions, spite the competition with arsenate is less intensive, the maximum of adsorption disappear in all cases and a plateau is reached by decreasing the adsorption capacity by three fold.

The decrease of adsorption capacity is used to quantify the interfering effect of the different anions at pH 4.0 (conditions for the higher adsorption capacity values). The obtained values are given in Table 1.

The observed interference level decreases as follows, phosphate \gg sulfate \sim nitrate \sim chloride. Therefore, the results show that the adsorption capacity is similar in the presence of all interfering anions except phosphate, which presents a more pronounced interfering effect. The high interference effect shown by phosphate in all pH range is due to both the effective competition for Fe(III) centers of the SPION, according to the similar affinity of phosphate and arsenate for Fe(III) and the higher concentration of phosphate versus arsenate [1].

The adsorption capacity in presence of interfering anions is less reduced when sulfate is present as interfering anions than when phosphate is the interfering due to the ligand exchange process in the system presents higher affinity when the anion has higher ionic charge.

The adsorption process increase when nitrate and chloride are present as interfering anions due to these anions have less interference in the ligand exchange process.

Finally, the effect of the phosphate in the remarkable decrease of the adsorption capacity of arsenic can be explained by the efficient competition with arsenic in the ligand exchange centers of the SPION for the complete pH range of study. This fact is consequence of the similar affinity of the phosphate and arsenate for Fe(III) centers and due to the higher phosphate concentration in relation with the arsenic concentration [1].

Table 1

Interfering effect of different anions on arsenate adsorption capacity at pH 4.0 with a molar ratio 1:200 of arsenic vs anions.

Sample	Adsorption capacity (mmol/g)	Decrease of adsorption capacity (%)
Without interference	12.09	–
Chloride	4.11	65.9
Nitrate	4.10	66.1
Sulfate	4.78	60.5
Phosphate	1.36	88.8
All interfering anions	1.71	85.9

3.8. Desorption experiments over Forager Sponge-loaded SPION

Corresponding results of the desorption process show high desorption degree when using 1.0 M HNO_3 (>99%) and 0.5 M H_3PO_4 (90%) for both As(III) and As(V) as shows Table 2. In addition, some desorbing species such as NaOH (1.0 M and 0.1 M) and H_3PO_4 become a problem for the adsorbent system due to these desorbents remove the SPION of the Sponge surface and degrade the SPION. Then, the adsorbent system loss the principal adsorbent compound and it cannot be used for new water treatments.

The desorption process by using chloride and hydroxide ions suggest that the interaction between the ions and the Fe(III) ions from the SPION is not enough strong to desorb both arsenite and arsenate. On the other hand, phosphoric acid, despite having the phosphate higher affinity to Fe(III) is not able to fully accomplish the desorption of arsenic. Finally, in the case of nitric acid, is the proton (H^+) which compete efficiently with Fe(III) from SPION to desorb the adsorbed arsenic species. When comparing phosphoric and nitric acid, the later one is stronger and then, present more free H^+ to react (1.0 M in the case of HNO_3 and 0.0576 M for H_3PO_4).

Table 2

Desorption percentage for different desorbing species.

Stripping solution	As(III) recovery (%)	As(V) recovery (%)	As(III–V) recovery (%)
NaOH 1.0 M	49.0	48.6	42.8
NaOH 0.1 M	31.6	38.9	34.3
NaOH 0.05 M	12.7	25.3	19.7
NaCl 2.0 M	37.0	54.1	39.4
NaCl 1.0 M	56.1	67.5	61.5
H_3PO_4 0.5 M	89.8	91.3	90.5
HNO_3 1.0 M	99.3	98.2	97.2

Table 3

Comparison of adsorbent materials adsorption capacity.

Adsorbent Material	As(V)		As(III)		pH	Ref.
	mmol/g SPION	mmol/g Fe	mmol/g SPION	mmol/g Fe		
SPION	0.91	1.25	0.43	0.71	3.8	
Forager Sponge loaded SPION	12.06	n/a	2.11	n/a	3.6	
Fe(III) loaded Forager Sponge	n/a	0.5	n/a	0.2	3.0	18
Fe(III) loaded resin	n/a	0.45	n/a	n/a	1.3–1.8	30
Hydrous iron oxide MNPs	0.51	n/a	n/a	n/a	4.5	31
Fe ₃ O ₄ @CTAB	0.31	n/a	n/a	n/a	3.0	32
Hydrous iron oxide	2.01	n/a	n/a	n/a	4.0	33
3-MPA-coated SPION	1.92	n/a	n/a	n/a	3.6	22
Adsorbent Material	As(V) (mmol/g)		As(III) (mmol/g)		pH	Ref.
Char-carbon (from fly-ash)	0.46		1.19		2.2	34
Activated carbon – Fe(III)	0.04		n/a		3.0	35
Chitosan-coated activated alumina	0.75		1.28		4.0	36
Fe–Ti bimetal oxide	1.13		0.19		4.0	37
Bimetal oxide magnetic CoFe ₂ O ₄	n/a		1.33		3.0	38
Mixed ferrite and hausmannite nanomaterials	0.55		0.19		3.0	39

Then, desorption of both arsenite and arsenate seems to be effective by ionic exchange but not by ligand exchange. By ligand exchange the interaction is stronger due to the exchange is produced in the inner sphere of coordination. Therefore, 1.0 M HNO₃ is the desorbing reagent that is most able to efficiently desorb without degrading the adsorbent system.

3.9. Adsorption capacity comparison with similar adsorbent systems

Comparing the obtained results, as shown by Table 3, with similar studies employing the same type of Forager Sponge loaded with Fe(III), a high difference adsorption is observed. To explain this behavior, it must be taken into account that the SPION provide more accessible centers for the arsenic adsorption respect the Fe(III). Forager Sponge loaded SPION is 35 times more effective for As(V) and 16 times higher for As(III) than SPION. SPION dispersion over the sponge surface provides a more active adsorption sites accessible to both arsenite and arsenate. Something similar happen in the case of different types of resins loaded with iron(III), where the SPION loaded sponge improves As(V) adsorption 19 times, while doubles the adsorption capacity of As(III). The most important reason for the observed increase of is the decrease of SPION aggregation by a dispersion that leads to a higher availability of adsorption positions [18,22,29–39].

When the comparison is made with nanoparticles, nanocomposites or adsorbent systems with different active centers, something similar happens. The two developed systems, non-supported, and Forager Sponge-loaded SPION present better adsorption capacity than the reported results in the literature.

4. Conclusions

Forager Sponge loaded SPION was successfully developed and optimized to obtain a new adsorbent system with a fine and homogeneous SPION layer over the Forager® Sponge surface with a reduced aggregation. The porosity and the obtained surface area by the milling process, makes that this support can provide the

optimal conditions to develop an important role for these water treatment applications.

The optimum adsorption parameters were evaluated and determined as in previous adsorbent systems. The SPION suspension studies, the new adsorbent system works in optimum conditions to recover arsenate at pH 3.6, while arsenite adsorption is not pH dependent and constant in a wide pH range. In case of Forager Sponge loaded SPION, the adsorption capacities are 2.11 mmol As/g SPION and 12.09 mmol As/g SPION for arsenite and arsenate, respectively, improving those achieved adsorption capacities for non-supported SPION.

It is noteworthy that Forager Sponge-Loaded SPION present an adsorption capacities around 6 mmol/g and 1.5 mmol/g for As(V) and As(III) respectively at pH 6.5. Therefore, the system not only can be applied for mining industrial water or other acidic water but can be used for actual drinking water treatment.

Acknowledgments

Project CTM2006-13091-C02-02/TECNO from the Ministerio de Ciencia e Innovación (Spanish Ministry for Science and Innovation) provided a grant to Diego Morillo to carry out the present work. Project SOWAEUMED (245843) FP7-REGPOT-2009-2.

References

- [1] J.M. Azcue, J.O. Nriagu, *Arsenic in the Environment. Part I: Cycling and Characterization*, in: J.O. Nriagu (Ed.), John Wiley & Sons, New York, 1994.
- [2] P.L. Smedley, D.G. Kinniburgh, *Appl. Geochem.* 17 (5) (2005) 517–568.
- [3] J.E. Fergusson, *The Heavy Metals: Chemistry, Environment Impact and Health Effects*, J.E. Fergusson, Pergamon Press, Oxford, 1990.
- [4] W.R. Penrose, *CRC Crit. Rev. Environ. Control* 4 (1974) 465–482.
- [5] USEPA, United States Environmental Protection Agency. Arsenic in drinking water; <<http://water.epa.gov/lawsregs/rulesregs/sdwa/arsenic/index.cfm>> (Consulted 21.11.10).
- [6] P. Kauppi, M.L. Räsänen, S. Myllyoja, *Finnish Environ.* 29 (2011) 1–219.
- [7] D.K. Nordstrom, *Appl. Geochem.* 26 (2011) 1777–1791.
- [8] Jie Cui, Yaguang Du, Hongxia Xiao, Qiushi Yi, Dongyun Du, *Hydrometallurgy* 146 (2014) 169–174.
- [9] D. Mohan, C.U. Pittman, *J. Hazard. Mater.* 142 (1–2) (2007) 1–53.
- [10] N. Valcarcel, A. Gómez, *Técnicas Analíticas de Separación*, Reverté S.A., Barcelona, 1990.
- [11] J.M. McNeil, D.E. McCoy, *Standard Handbook of Hazardous Waste Treatment and Disposal*, McGraw Hill book Company, New York, 1999, p. 6.91.
- [12] J.M. McNeil, D.E. McCoy, *Standard Handbook of Hazardous Waste Treatment and Disposal*, McGraw Hill book Company, New York, 1999, p. 6.3.
- [13] T. Sakalakis, *NATO Sci. Ser., II: Math. Phys. Chem. (Nanostruct.: Synth., Funct. Prop. Appl.)* 1 (2003) 128.
- [14] G.F. Goya, T.S. Berquo, F.C. Fonseca, *J. Appl. Phys.* 94 (2003) 3520–3528.
- [15] T. Tuutijärvi, J. Lu, M. Sillanpää, G. Chen, *J. Hazard. Mater.* 166 (2–3) (2009) 1415–1420.
- [16] J. Jönsson, D.M. Sherman, *Chem. Geol.* 255 (2008) 173–181.
- [17] H.J. Shipley, S. Yean, A.T. Kan, M.B. Tomson, *Environ. Toxicol. Chem.* 28 (3) (2009) 509–515.
- [18] J.A. Muñoz, A. Gonzalo, M. Valiente, *Environ. Sci. Technol.* 36 (2002) 3405–3411.
- [19] N.L. Adolphi, *J. Magn. Magn. Mater.* 321 (2009) 1459–1464.
- [20] M. Garza, M. Hinojosa, V. Gonzalez, *Desarrollo de nanocomposites superparamagneticos de matriz biopolimérica*, CIENCIA UANL, Abril-Junio, Vol XII (2), 2009.
- [21] K.H. Kim, *IEEE Trans. Magn.* 44 (11) (2008) 2940–2943.
- [22] D. Morillo, A. Uheida, G. Pérez, M. Muhammed, M. Valiente, *J. Colloid Interface. Sci.* 438 (2015) 227–234.
- [23] A. Uheida, G. Salazar-Alvarez, E. Björkman, Y. Zhang, M. Muhammed, *J. Colloid Interface Sci.* 298 (2006) 501–507.
- [24] A.B. Chin, I.I. Yacob, *J. Mater. Process. Technol.* 191 (2007) 235–237.
- [25] L.G. Sillén, A.E. Martell, *Stability Constants, Special Publications No. 17*, The Chemical Society, London, 1964.
- [26] J.S. Arribas, F. Burriel, J.H. Méndez, F.L. Conde, *Química Analítica Cualitativa*, Ed. Paraninfo, 2006.
- [27] I. Puigdomenech, *Medusa*, Royal Institute of Technology, Estocolm, 1999 <www.inorg.kth.se> (Software).
- [28] D.K. Bhumbla, R.F. Keefer, *Arsenic in the Environment. Part I: Cycling and Characterization*, in: J.O. Nriagu (Ed.), John Wiley & Sons, New York, 1994, p. 51.
- [29] N.B. Rainer, *Process for the selective absorption of anions*, US PATENT 5,187,200, 1993.
- [30] I. Rau, A. Gonzalo, M. Valiente, *React. Funct. Polym.* 54 (2003) 85–94.

- [31] T. Pradeep, *Thin Solid Films* 517 (24) (2009) 6441–6478.
- [32] Y. Jin, F. Liu, M. Tong, Y. Hou, *J. Hazard. Mater.* 227–228 (2012) 461–468.
- [33] T.-H. Hsia, S.-L. Lo, C.-F. Lin, D.-Y. Lee, *Colloids Surf. A* 85 (1994) 1–7.
- [34] J. Pattanayak, K. Mondal, S. Mathew, S.B. Lalvani, *Carbon* 38 (4) (2000) 589–596.
- [35] A.O.A. Tuna, E. Ozdemir, E.B. Simsek, U. Beker, *Chem. Eng. J.* 223 (2013) 116–128.
- [36] J.M. Hao, M.J. Han, X.G. Meng, *J. Hazard. Mater.* 167 (1–3) (2009) 1215–1221.
- [37] K. Gupta, U.C. Ghosh, *J. Hazard. Mater.* 161 (2–3) (2009) 884–892.
- [38] S.X. Zhang, H.Y. Niu, Y.Q. Cai, X.L. Zhao, Y.L. Shi, *Chem. Eng. J.* 158 (3) (2010) 599–607.
- [39] S. Garcia, S. Sardar, S. Maldonado, V. Garcia, C. Tamez, J.G. Parsons, *Microchem. J.* 117 (2014) 52–60.